



Cite this: DOI: 10.1039/c9tb02794g

Received 10th December 2019,
Accepted 13th February 2020

DOI: 10.1039/c9tb02794g

rsc.li/materials-b

A rhodol-enone dye platform with dual reaction triggers for specific detection of Cys†

Linan Hu,^{ab} Zhu Chen,^a Cheng Yu,^a Jie Zhang,^a Hailiang Zhang,^c Pengfei Xu^{id}*^c
and Enhua Xiao*^a

Cys is a common and important sulfur-containing amino acid in living organisms, whose intracellular level changes are associated with a variety of diseases. In order to specifically detect Cys without interference from other thiol species, we have developed a rhodol-enone dye platform (termed as probe **BL-C**) with an acrylate group and an α,β -unsaturated ketone as bis-reaction-triggers. Our probe **BL-C** can remarkably exhibit a turn on signal towards Cys with high selectivity. Moreover, it has been successfully applied for detection of cysteine in living cells in terms of its excellent cell permeability. In conclusion, these desirable characteristics indicate that probe **BL-C** could be applied to discriminative sensing of intracellular Cys in biological applications.

1. Introduction

Biological thiols (biothiols), such as cysteine (Cys), homocysteine (Hcy) and glutathione (GSH), play many crucial roles in physiological and pathological processes.¹ A series of important enzymes and proteins are involved in the metabolism and transportation of Cys, Hcy and GSH in biological systems. Thus, endogenous concentrations of these thiols properly reflect the functional state of the corresponding enzymes and proteins and their abnormal levels correlate with diseases.^{2,3} For example, in the normal state, intracellular level of Cys in human metabolism is in the range of 30 to 200 μM , and abnormal levels of Cys are associated with several diseases.^{4,5} The lack of Cys is reported to cause decreased hematopoiesis, leukocyte loss, neurotoxicity, slow growth in children, liver damage, and Parkinson's disease. In contrast, an elevated amount of Cys can lead to cardiovascular issues, Alzheimer's disease, and inflammatory bowel disease.^{6–8} Therefore, an efficient method for selectively probing for Cys in biological systems is urgently required for better understanding of its biological functions and for the early diagnosis of some diseases.

Fluorescent probes have been recognized as the most efficient molecular tools, which can help visualize trace amounts of targeted biomolecules in biological systems due to their simplicity,

sensitivity, real-time imaging, and nondestructive detection characteristics.^{9–13} So far, various fluorescent probes have been developed for the detection of Cys.^{14–16} Most of these probes were designed to exploit the strong nucleophilicity of the sulfhydryl group, which enables reactions such as the Michael addition, and the cleavage of sulfonamides, sulfonate esters, and S–S bonds. Unfortunately, these probes are unable to discriminate Cys from other biothiol species. In order to achieve better selectivity, the amino or carboxylic acid group was also involved in the sensing processes. For example, the aldehyde group and acrylate group have been used as the discrimination groups. Although good to excellent selectivity could generally be achieved between Cys/Hcy and GSH, only modest selectivity could be realized between Cys and Hcy due to their minute structural difference.^{17–19} As illustrated in Scheme 1, the thiol-Michael addition between an acrylate group and a biothiol generates the corresponding thioether, and a subsequent intramolecular cyclization and further self-immolation yield 7-*exo*-trig for Cys and 8-*exo*-trig for Hcy, according to Baldwin's nomenclature.^{14,20} Similarly, aldehydes can react with the N-terminus of Cys and Hcy to form thiazolidines and thiazinanes, respectively.^{14,21–23} Thus, the selectivity all depends on the reaction kinetics differences in the formation of the ring and is difficult to improve by a single recognition group. Therefore, it still remains a huge challenge to determine the intracellular concentration of Cys accurately without the interference of other thiol species.

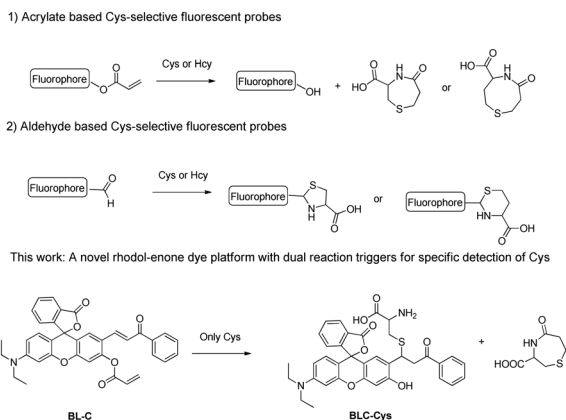
In this work, we design and synthesize a novel fluorescent probe with dual reaction triggers to enhance the detection specificity for Cys.^{24,25} At first, we need to choose an excellent fluorophore to synthesize the bis-reaction-trigger probe. It is well known that phenolic oxygen containing xanthene dyes

^a Department of Radiology, The Second Xiangya Hospital, Central South University, Changsha, Hunan 410011, P. R. China

^b Department of Radiology, Zhuzhou Central Hospital, Zhuzhou, Hunan 412000, P. R. China

^c Institute of Clinical Pharmacy & Pharmacology, Jining First People's Hospital, Jining Medical University, Jining 272000, P. R. China

† Electronic supplementary information (ESI) available. See DOI: 10.1039/c9tb02794g



Scheme 1 Schematic illustration of a single fluorophore with dual reaction triggers for the specific detection of Cys.

such as rhodol are usually used for the design of probes for many analytes.^{26–29} Rhodol is usually present in equilibrium between the “open” fluorescent quinoid form and the “closed” nonfluorescent spirolactone, which would allow us to optimize the photophysical properties of rhodol dyes for the desired applications by reasonable modification. On the other hand, it is well known that when a dye possesses an electron rich group conjugated to an electron deficient group, intramolecular charge transfer (ICT) from the donor to the acceptor will proceed upon excitation. ICT is an effective mechanism to tune the photophysical properties of fluorophores. In this work, we synthesized a novel dye **BL** by introducing an enone unit adjacent to the phenolic oxygen aimed at extending the π -conjugation of rhodol. To our delight, the dye **BL** displayed obvious redshifts in its absorption (abs: 560 nm) and emission (em: 600 nm) wavelengths, when compared with those of its rhodol parent. Interestingly, the fluorescent peak of **BL** shifted from 600 nm to 560 nm after treatment with Cys because of the break in the conjugated structure by Cys. As such, the enone group can be utilized as a reaction site for cys. In order to design a bis-reaction-trigger probe, acrylate, which has been proved to be a highly selective and rapid (within 3 min) quenching and recognizing moiety for Cys, was selected as another reaction site. In the presence of Cys, the reaction between the acrylate group and Cys generates the corresponding thioether, and a subsequent intramolecular cyclization and further self-immolation yield the lactam byproduct and **BL** with a strong fluorescence. Thus, by using an acrylate group and an enone group as dual-reaction sites, probe **BL-C** will exhibit high selectivity towards Cys.

2. Experimental sections

2.1. Materials and methods

All commercial chemicals were purchased from commercial suppliers and used without further purification. All solvents were purified before use. The liver cancer cell line HepG2 was purchased from the Type Culture Collection of the Chinese Academy of Sciences, Shanghai, China. Dulbecco's modified Eagle's medium (DMEM) was purchased from Sigma-Aldrich.

Other medium components were obtained from Sigma-Aldrich too. Fetal bovine serum (FBS) was obtained from Hyclone Laboratories Inc. Fluorescence imaging of HepG2 cells was carried out using an Olympus FV1000 confocal fluorescence microscope. ¹H NMR and ¹³C NMR spectra were obtained on a Bruker Ascend 400 NMR spectrometer. Electrospray ionization mass spectra (ESI-MS) were collected on an Agilent 6460 triple quadrupole LC/MS instrument. Absorbance spectra were recorded on a Shimadzu UV-2450 UV-visible spectrophotometer. Fluorescence emission and excitation spectra were measured using a Hitachi F-7000 spectrofluorometer.

2.2. Synthesis details

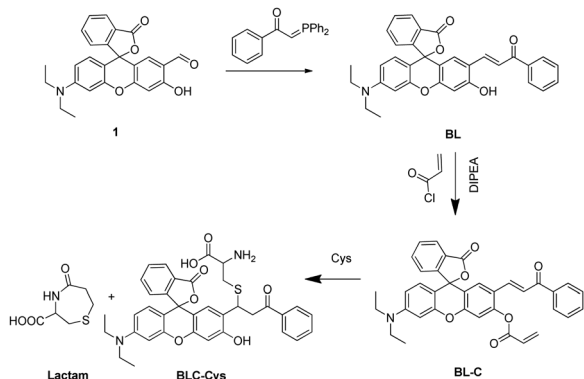
Synthesis and characterization of BL. Compound **1** (415 mg, 1.0 mmol), 1-phenyl-2-(triphenylphosphoranylidene) ethenone and dichloromethane (15 mL) were added to a 50 mL round bottomed flask. Then, the mixture was stirred under a N₂ atmosphere at room temperature. The reaction was monitored using TLC analysis and it was completed in 10 hours. The reaction mixture was concentrated *in vacuo* and the residue was purified by silica gel chromatography (methanol:dichloromethane = 1:12 v/v) to give a purple solid **BL** (367 mg, 61% yield).

Synthesis and characterization of probe BL-C. Acryloyl chloride (54 mg, 0.6 mmol) was added dropwise to a solution of **BL** (258 mg, 0.5 mmol) and Et₃N (83 μ L, 0.6 mmol) in anhydrous CH₂Cl₂ (10 mL) at 0 °C. Stirring was continued at this temperature for half an hour, and then the resulting mixture was further stirred for 10 h at room temperature. Water (10 mL) was added to the mixture, followed by extraction with CH₂Cl₂ (15 mL \times 3). The combined organic phase was dried by anhydrous Na₂SO₄. The solvent was removed by evaporation, and the residue was purified by flash column chromatography on silica gel to afford probe **BL-C** as a colorless solid (237 mg, 83%). ¹H NMR (600 MHz, chloroform-*d*) δ 8.06 (d, *J* = 7.6 Hz, 1H), 7.88–7.84 (m, 2H), 7.70 (d, *J* = 7.5 Hz, 1H), 7.67–7.65 (m, 1H), 7.63 (d, *J* = 4.8 Hz, 1H), 7.54 (d, *J* = 6.9 Hz, 1H), 7.44 (t, *J* = 7.6 Hz, 2H), 7.24 (d, *J* = 7.5 Hz, 1H), 7.19–7.11 (m, 3H), 6.69 (d, *J* = 17.4 Hz, 1H), 6.58 (d, *J* = 8.9 Hz, 1H), 6.46 (d, *J* = 2.6 Hz, 1H), 6.41–6.31 (m, 2H), 6.11 (d, *J* = 10.5 Hz, 1H), 3.36 (q, *J* = 7.0 Hz, 4H), 1.17 (t, *J* = 7.1 Hz, 6H). ¹³C NMR (151 MHz, CDCl₃) δ 190.49, 169.47, 163.62, 153.45, 152.81, 152.41, 150.55, 149.73, 137.88, 137.51, 135.20, 134.09, 132.82, 129.94, 128.79, 128.60, 128.53, 127.13, 126.80, 125.20, 124.09, 123.70, 123.50, 118.40, 111.79, 108.99, 104.76, 97.75, 83.09, 44.57, 12.48. ESI-MS: *m/z* 572.2 [M + H]⁺.

3. Results and discussion

3.1. Synthesis of probe BL-C

The synthetic route of probe **BL-C** is shown in Scheme 2. Compound **1** can be easily achieved as in previous reports,³⁰ which was treated with 1,3,3-triphenylprop-2-en-1-one to afford probe **BL**. Probe **BL-C** was easily prepared by the reaction of compound **BL** and acryloyl chloride in the presence of triethylamine, and this fluorescent probe exhibited negligible fluorescence. The chemical structure of probe **BL-C** was identified



Scheme 2 The synthesis route of probe **BL-C** and its proposed detection mechanism.

using NMR and mass spectrometry. This design was based on the following rationale: (1) the emission of rhodol derivatives was red-shifted to 600 nm by extending the π -conjugation backbone; (2) a Michael addition can take place between the enone group and Cys; (3) acrylate can also work as a reliable Cys selective trigger.

3.2. Spectral properties of BL

First, the photo-spectral properties of **BL** in PBS buffer (20 mM, pH 7.4) solution (ACN/water = 1/1, v/v) were explored. As shown in Fig. S9 (ESI[†]), the treatment with 10 equivalents of Cys caused a dramatic emission peak change. The emission peak centered at 600 nm blue-shifted to 560 nm. This is because upon adding Cys to the solution of **BL**, the nucleophilic Cys would attack the conjugated C=C double bond in **BL** via Michael type additions and destroy the conjugated molecule backbone.

3.3. Spectral properties of BL-C

The UV-vis and fluorescence spectra of **BL-C** in the absence or presence of Cys were also measured. As shown in Fig. 1, the solution of **BL-C** was colorless with no obvious absorption peak in the range of 450–650 nm. Upon the addition of Cys (1 equiv.), the predominant absorption peak centered at 560 nm and a shoulder peak around 520 nm were observed. Upon addition of another 9 equivalents of Cys, the absorption band at 520 nm

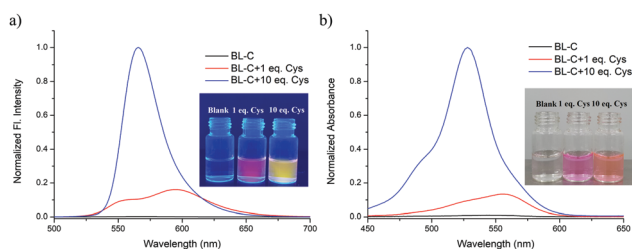


Fig. 1 (a) The normalized fluorescence spectra of **BL-C** (10 μ M) in the absence and presence of Cys (10 μ M and 100 μ M). Inset: Emission color changes of probe **BL-C** in the absence and presence of Cys (10 μ M and 100 μ M) under excitation with UV light (365 nm). (b) The normalized UV-vis absorption spectra of **BL-C** (10 μ M) in the absence and presence of Cys (10 μ M and 100 μ M). Inset: Visual color changes of probe **BL-C** in the absence and presence of Cys (10 μ M and 100 μ M).

increased dramatically. Correspondingly, the solution of **BL-C** displayed distinct color changes from colorless to purple and then to orange red, which could be easily observed with the naked eye (Fig. S9, ESI[†]). In the fluorescence spectra, the free probe **BL-C** showed nearly no fluorescence under excitation at 480 nm. However, after reacting with different concentrations of Cys (1 equiv. and 10 equiv.), the fluorescence signal of probe **BL-C** showed remarkable changes. As shown in Fig. 1a, upon addition of Cys (1 equiv.), a new emission peak around 600 nm with a shoulder peak around 560 nm was observed. In the presence of 10 equivalents of Cys, the fluorescence intensity of the emission peak at 560 nm increased dramatically.

3.4. Spectral response of BL-C to different concentration ranges of Cys

Next, we investigated the response capacity of **BL-C** to different concentrations of Cys (0–150 μ M). As shown in Fig. 2, in the absence of Cys, almost no fluorescence signal was observed. When the probe **BL-C** was treated with different concentrations of cys (0–30 μ M), the emission peak centered at 600 nm and the shoulder peak around 560 nm increased progressively. In the presence of a high concentration of Cys (40–150 μ M), the fluorescence intensity of the emission peak at 560 nm increased dramatically, which is 5-fold higher than that of 600 nm. The UV-vis absorbance responses of **BL-C** toward Cys has a similar characteristic. Briefly, in the absence of Cys, almost no absorbance peak in the range of 400–650 nm was observed. Upon gradual addition of Cys over a concentration range of 0–30 μ M, the main absorbance peak around 560 nm and the shoulder peak around 525 nm increased progressively. With further addition of Cys, the absorbance peak at 525 nm increased dramatically. This response profile implies that **BL-C** has different reaction pathways towards Cys. The first reaction pathway of **BL-C** responding to Cys is an addition-cleavage process. This process is based on the conjugated addition of Cys to a terminal acrylate group, which generates the intermediate thioether, and intramolecular cyclization giving the desired lactam and compound **BL**. The other reaction pathway was the conjugate 1,4-addition of thiol to α,β -unsaturated ketone forming a thioether **BL-Cys** adduct and breaking the π -conjugation of **BL**. The mass spectrometry analysis of probe **BL-C** titration with Cys confirms the formation of **BL** and a

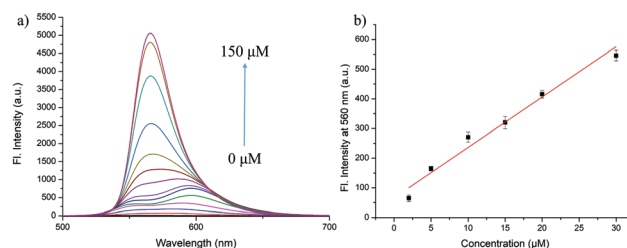


Fig. 2 (a) Fluorescence responses of probe **BL-C** (10 μ M) toward different concentrations of Cys (0–150 μ M) with $\lambda_{ex} = 480$ nm. (b) Fluorescence intensity at 560 nm of probe **BL-C** versus Cys concentration (0–30 μ M) with $\lambda_{ex} = 480$ nm. Error bars, SD ($n = 3$).

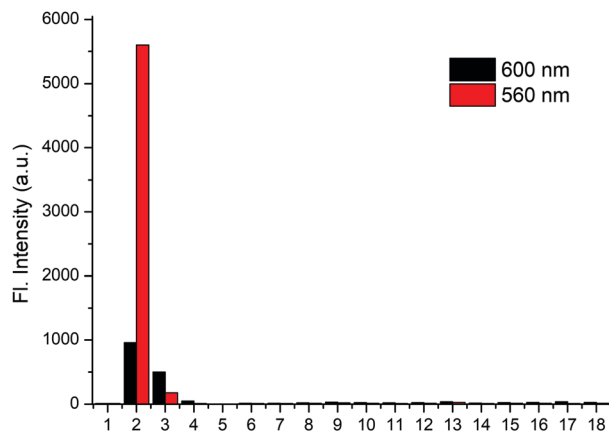


Fig. 3 Fluorescence changes of **BL-C** (10 μ M, $\lambda_{\text{ex}} = 480$ nm) with various analytes (200 μ M) at 600 nm and 560 nm, respectively. (1) Blank, (2) Cys, (3) Hcy, (4) GSH, (5) Gly, (6) Phe, (7) Ser, (8) Glu, (9) Lys, (10) Arg, (11) His, (12) Ala, (13) Gln, (14) Met, (15) Tyr, (16) HS⁻, (17) SO₃²⁻, and (18) S₂O₃²⁻. Each spectrum was recorded at 60 min after the addition.

BL-C-Cys adduct (Fig. S7, ESI⁺). The peak of the formed lactam was also observed (Fig. S8, ESI⁺). Moreover, the addition reaction of Cys with the acrylate group has a higher reaction rate than that of the reaction with α,β -unsaturated ketone. From the above, we can conclude that this novel probe **BL-C** has the particular dual-modes of fluorescence signals towards Cys.

3.5. Specificity of the probe **BL-C** to different bio-thiol species

To verify the selectivity of **BL-C** for Cys, we measured the fluorescence signal changes at both 600 nm and 560 nm after treatment with various biological species (Fig. 3). Only Cys could induce obvious fluorescence enhancement at 560 nm. Compared with other interferents, Hcy with probe **BL-C** exhibited slightly enhanced fluorescence at 600 nm and 560 nm. However, the ratio of emission intensities at 560 nm, respectively, induced by Cys and Hcy ($I_{560}^{\text{Cys}}/I_{560}^{\text{Hcy}}$) is 34, which is 17 times higher than that at 600 nm ($I_{600}^{\text{Cys}}/I_{600}^{\text{Hcy}}$). Moreover, the concentration of Hcy is at least ten times lower than that of Cys in normal plasma. These results indicated that the probe **BL-C** can distinguish Cys specifically,

suggesting that the probe **BL-C** has wonderful potential applications in the studies of biological fields.

3.6. Fluorescence imaging of Cys in living cells

Encouraged by the fluorescence change and the good selectivity toward Cys, we next investigated the biological applications of the probe **BL-C**. The nuclei of HepG2 cells were stained by DAPI (4',6-diamidino-2-phenylindole) and imaged in blue channels. As shown in Fig. 4, living HeLa cells were incubated with **BL-C** at 37 °C for 60 min, and outstanding green fluorescence was observed in the cytoplasm with excitation at 485 nm. In the control experiment, the cells were pretreated with the thiol-blocking reagent *N*-ethylmaleimide (NEM, 2 mM) for 30 min and then co-incubated with the probe **BL-C** for 60 min. As shown in Fig. 4, nearly no fluorescence in the green channels was observed with excitation at 485 nm. In summary, the results indicate that the probe **BL-C** possesses great potential for biological applications.

4. Conclusion

In summary, we have developed a rhodol-enone dye platform with bis-reaction-triggers for the selective detection of Cys. The key point of our design is to equip the probe with two reaction triggers on the appropriate sites that determine its emissive properties when treated with Cys. Furthermore, by extending the π -conjugation of rhodol, the rhodol-enone dye **BL** exhibits red emission at 600 nm. By using an acrylate group and enone group as dual-reaction sites, the probe **BL-C** exhibited high selectivity towards Cys. Both of the imaging experiments carried out in aqueous solution and in live cells have confirmed the potential of the probe **BL-C** for specific detection of Cys. These results suggest that the probe **BL-C** has promising prospects for biological applications.

Conflicts of interest

There are no conflicts to declare.

Acknowledgements

This work was financially supported by the National Natural Science Foundation of China (No. 81701754 and 81601471) and the Provincial Natural Science Foundation of Hunan (No. 2019JJ40434).

Notes and references

- 1 S. Zhang, C. N. Ong and H. M. Shen, *Cancer Lett.*, 2004, **208**, 143–153.
- 2 S. M. Marino and V. N. Gladyshev, *J. Mol. Biol.*, 2010, **404**, 902–916.
- 3 C. E. Paulsen and K. S. Carroll, *Chem. Rev.*, 2013, **113**, 4633–4679.
- 4 C. Hwang, A. J. Sinskey and H. F. Lodish, *Science*, 1992, **257**, 1496–1502.

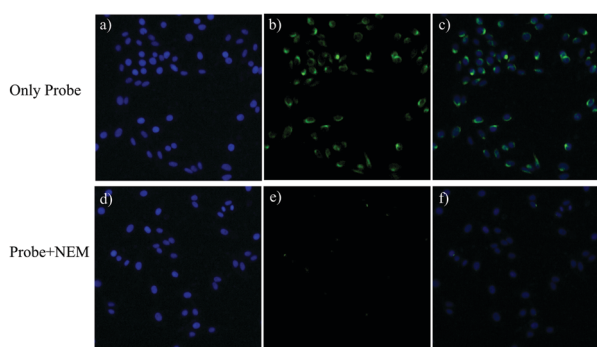


Fig. 4 Confocal microscopy images of the probe **BL-C** in HepG2 cells co-stained with 4',6-diamidino-2-phenylindole (DAPI) to identify cell nuclei (blue dots). (a and d) Fluorescence images from DAPI; (b and e) fluorescence images from **BL-C**; (c and f) merge.

- 5 S. Park and J. A. Imlay, *J. Bacteriol.*, 2003, **185**, 1942–1950.
- 6 L. A. Herzenberg, S. C. De Rosa, J. G. Dubs, M. Roederer, M. T. Anderson, S. W. Ela, S. C. Deresinski and L. A. Herzenberg, *Proc. Natl. Acad. Sci. U. S. A.*, 1997, **94**, 1967–1972.
- 7 W. Lin, L. Long, L. Yuan, Z. Cao, B. Chen and W. Tan, *Org. Lett.*, 2008, **10**, 5577–5580.
- 8 S. Shahrokhian, *Anal. Chem.*, 2001, **73**, 5972–5978.
- 9 L. Albertazzi, D. van der Zwaag, C. M. Leenders, R. Fitzner, R. W. van der Hofstad and E. W. Meijer, *Science*, 2014, **344**, 491–495.
- 10 J. Chan, S. C. Dodani and C. J. Chang, *Nat. Chem.*, 2012, **4**, 973–984.
- 11 M. Fessenden, *Nature*, 2016, **533**, 565–568.
- 12 E. L. Sylwestrak, P. Rajasethupathy, M. A. Wright, A. Jaffe and K. Deisseroth, *Cell*, 2016, **164**, 792–804.
- 13 A. M. Valm, S. Cohen, W. R. Legant, J. Melunis, U. Hershberg, E. Wait, A. R. Cohen, M. W. Davidson, E. Betzig and J. Lippincott-Schwartz, *Nature*, 2017, **546**, 162–167.
- 14 L. Y. Niu, Y. Z. Chen, H. R. Zheng, L. Z. Wu, C. H. Tung and Q. Z. Yang, *Chem. Soc. Rev.*, 2015, **44**, 6143–6160.
- 15 N. Wang, Y. Wang, J. Gao, X. Ji, J. He, J. Zhang and W. Zhao, *Analyst*, 2018, **143**, 5728–5735.
- 16 C. Yin, F. Huo, J. Zhang, R. Martinez-Manez, Y. Yang, H. Lv and S. Li, *Chem. Soc. Rev.*, 2013, **42**, 6032–6059.
- 17 S. Q. Wang, Q. H. Wu, H. Y. Wang, X. X. Zheng, S. L. Shen, Y. R. Zhang, J. Y. Miao and B. X. Zhao, *Biosens. Bioelectron.*, 2014, **55**, 386–390.
- 18 X. Yang, Y. Guo and R. M. Strongin, *Angew. Chem., Int. Ed.*, 2011, **50**, 10690–10693.
- 19 Q. Zhang, D. Yu, S. Ding and G. Feng, *Chem. Commun.*, 2014, **50**, 14002–14005.
- 20 X. Li, Y. Zheng, H. Tong, R. Qian, L. Zhou, G. Liu, Y. Tang, H. Li, K. Lou and W. Wang, *Chemistry*, 2016, **22**, 9247–9256.
- 21 A. Barve, M. Lowry, J. O. Escobedo, K. T. Huynh, L. Hakuna and R. M. Strongin, *Chem. Commun.*, 2014, **50**, 8219–8222.
- 22 M. Hu, J. Fan, H. Li, K. Song, S. Wang, G. Cheng and X. Peng, *Org. Biomol. Chem.*, 2011, **9**, 980–983.
- 23 M. Tian, F. Guo, Y. Sun, W. Zhang, F. Miao, Y. Liu, G. Song, C. L. Ho, X. Yu, J. Z. Sun and W. Y. Wong, *Org. Biomol. Chem.*, 2014, **12**, 6128–6133.
- 24 D. Li, J. Cheng, C. K. Wang, H. Ying, Y. Hu, F. Han and X. Li, *Chem. Commun.*, 2018, **54**, 8170–8173.
- 25 P. Wang, Q. Wang, J. Huang, N. Li and Y. Gu, *Biosens. Bioelectron.*, 2017, **92**, 583–588.
- 26 Y. Fang, G. N. Good, X. Zhou and C. I. Stains, *Chem. Commun.*, 2019, **55**, 5962–5965.
- 27 J. Guan, Q. Tu, L. Chen, M. S. Yuan and J. Wang, *Spectrochim. Acta, Part A*, 2019, **220**, 117114.
- 28 X. Jin, J. Gao, T. Wang, W. Feng, R. Li, P. Xie, L. Si, H. Zhou and X. Zhang, *Spectrochim. Acta, Part A*, 2020, **224**, 117467.
- 29 K. N. More, T. H. Lim, J. Kang, H. Yun, S. T. Yee and D. J. Chang, *Molecules*, 2019, **24**, 3206–3222.
- 30 Y. Zhang, L. Ma, C. Tang, S. Pan, D. Shi, S. Wang, M. Li and Y. Guo, *J. Mater. Chem. B*, 2018, **6**, 725–731.